

TVD adaptive mesh redistribution scheme for the shallow-water equations

M. Louaked^{*,†}

Laboratoire de Mathématiques Nicolas Oresme, Université de Caen, Bd du Maréchal Juin, 14032 Caen Cedex, France

SUMMARY

This work presents a high-resolution scheme combined with a moving mesh method for approximating the solution of shallow water system. The main difficulties in deriving stable and convergent numerical approximations can be due to solutions that vanish in nontrivial parts of domain such as dry states in water flows. In these situations, the coupling between characteristic fields gradually increases as water height is stepped down. The basic methodology in our method is to avoid characteristic decompositions in the spatial discretization. Moving dry regions within the computing domain are captured without the appearance of negative values. The high-resolution properties of the scheme as well as its resistance to mesh orientation gives the great potential of the moving mesh methods for reducing computational costs without sacrificing the overall level of accuracy, which is demonstrated in a variety of hydraulic examples. Copyright © 2007 John Wiley & Sons, Ltd.

Received 27 April 2007; Revised 10 September 2007; Accepted 12 September 2007

KEY WORDS: shallow-water system; TVD high-resolution scheme; moving mesh

1. INTRODUCTION

Shallow-water equations (SWEs) are used to describe coastal, estuarine and inland water flows under the action of gravity force. SWEs express a nonhomogeneous system of conservation laws in terms of local water height and discharge.

Designing an efficient and robust numerical method for this model is a stimulating task: solutions are typically nonsmooth, they may contain hydraulic jumps and flood waves. In addition, many real applications introduce further complications such as variable topography and evolving dry regions within the domain. Dealing with dry bed situations needs special attention. The difficulty arises from the fact that the coupling between characteristic fields in SWE increases as the water

*Correspondence to: M. Louaked, Laboratoire de Mathématiques Nicolas Oresme, Université de Caen, Bd du Maréchal Juin, 14032 Caen Cedex, France.

†E-mail: louaked@math.unicaen.fr

height decreases. This increased coupling is a reflection of the fact that strict hyperbolicity is lost and the eigenvalues and eigenvectors coalesce at the dry regions.

In recent years, major progress has been made in numerical aspects of the field and several high-resolution schemes have been suggested in the literature to approximate the shallow-water system [1, 2]. Many of these modern approximations employ a set of eigenvalues of the Jacobian matrix and an appropriate linearized characteristic decomposition. For all the reasons cited above, this class of schemes may fail near or with dry conditions.

In this work, we present a method that is highly efficient to compute flows over wet or dry surfaces. A TVD component-wise limiting strategy is designed to restrict or suppress oscillations near discontinuities. The spatial discretization is a Riemann-solver-free recipe and field-by-field decompositions are avoided.

The principal feature of nonlinear shallow-water system, manifested in the physical phenomenon of breaking of waves, is the breakdown of classical solutions and the development of discontinuities that propagate as hydraulic jumps. This leads us to try to concentrate the computational effort where it is needed most. For problems in these areas, very fine meshes are often required over a small portion of the physical domain to resolve large solution variations there.

Significant improvements in accuracy and efficiency can be gained by using moving mesh methods for problems having large solution variations. The moving mesh approach is to keep a fixed numbers of mesh points and to move them according to a prescribed algorithm.

Numerical results are given to illustrate the accuracy of the method.

The structure of the paper is as follows. The next section presents the SWEs in general coordinates. Section 3 deals with the high-resolution scheme. The moving mesh method and its implementation are described in Section 4. The results of the numerical experiments are presented in Section 5. Finally, Section 6 concludes the paper.

2. GOVERNING EQUATIONS

SWEs form a depth-integrated model for free surface flow of a fluid under the influence of gravity. In the model, it is assumed that the surface perturbation is much smaller than the typical horizontal length scale.

Since the computation is carried out in the computational plan, the shallow-water system can be cast in the strong conservation law form in the computational $\xi - \eta$ plan as

$$\frac{\partial}{\partial t} \left(\frac{U}{J} \right) + \frac{\partial \tilde{F}}{\partial \xi} + \frac{\partial \tilde{G}}{\partial \eta} = 0 \quad (1)$$

where

$$\tilde{F} = y_\eta F - x_\eta G, \quad \tilde{G} = -y_\xi F + x_\xi G, \quad J = (x_\xi y_\eta - x_\eta y_\xi)^{-1} \quad (2)$$

$$U = \begin{bmatrix} h \\ hu \\ hv \end{bmatrix}, \quad F = \begin{bmatrix} hu \\ hu^2 + \frac{1}{2}gh^2 \\ huv \end{bmatrix}, \quad G = \begin{bmatrix} hv \\ huv \\ hv^2 + \frac{1}{2}gh^2 \end{bmatrix} \quad (3)$$

$Q = (uh, vh)$ is the unit-width discharge and g is the gravitational acceleration.

3. THE HIGH-RESOLUTION SCHEME—A MODIFIED FLUX APPROACH

3.1. Wave equation

Consider the scalar wave equation:

$$u_t + au_\xi = 0, \quad a > 0 \quad (4)$$

Let u_j^n be the numerical solution of (4) at $\xi = j\Delta\xi$, $t = n\Delta t$ with $\Delta\xi$ the spatial mesh size and Δt the time step.

Following Sweby [3], the Lax–Wendroff method is written to look like an upwind part with an additional limited amount of anti-diffusive flux

$$u_j^{n+1} = u_j^n - \lambda \left\{ 1 + \frac{1}{2}(1-\lambda) \left[\frac{\phi(r_j^+)}{r_j^+} - \phi(r_{j-1}^+) \right] \right\} \Delta u_{j-1/2}^n \quad \text{with } r_j^+ = \frac{\Delta u_{j-1/2}^n}{\Delta u_{j+1/2}^n} \quad (5)$$

Here

$$\lambda = \frac{a\Delta t}{\Delta\xi}, \quad \Delta u_{j+1/2}^n = u_{j+1}^n - u_j^n \quad \text{and} \quad \Delta u_{j-1/2}^n = u_j^n - u_{j-1}^n$$

The flux limiter ϕ is defined under Harten's TVD inequalities [4].

3.2. Nonlinear scalar case

This approach of high resolution with flux limiter is extended to nonlinear scalar case in the framework of Sweby [3]. An explicit conservative difference scheme

$$u_j^{n+1} = u_j^n - \lambda(h_{j+1/2} - h_{j-1/2}) \quad (6)$$

serves as a consistent approximation to scalar conservation law

$$u_t + f(u)_\xi = 0 \quad (7)$$

Let

$$(\Delta f_{j+1/2})^+ = f(u_{j+1}) - g_{j+1/2}^E, \quad (\Delta f_{j+1/2})^- = f(u_j) - g_{j+1/2}^E \quad (8)$$

and

$$r_j^+ = (\Delta f_{j-1/2})^+ / (\Delta f_{j+1/2})^+, \quad r_j^- = (\Delta f_{j+1/2})^- / (\Delta f_{j-1/2})^- \quad (9)$$

Here g^E is the flux of any E-scheme, i.e. it is Lipschitz continuous, and for all u 's between u_j and u_{j+1} , it satisfies $\text{sgn}(u_{j+1} - u_j)(g_{j+1/2}^E - f(u)) \leq 0$. The numerical flux $h_{j+1/2}$ with the limiter ϕ is defined by

$$h_{j+1/2} = g_{j+1/2}^E + \frac{1}{2}\phi(r_j^+)\alpha_{j+1/2}^+(\Delta f_{j+1/2})^+ - \frac{1}{2}\phi(r_{j+1}^-)\alpha_{j+1/2}^-(\Delta f_{j+1/2})^- \quad (10)$$

with $\alpha_{j+1/2}^+ = \frac{1}{2}(1 - v_{j+1/2}^+)$, $\alpha_{j+1/2}^- = \frac{1}{2}(1 + v_{j+1/2}^-)$, and $v_{j+1/2}^+$, $v_{j+1/2}^-$ are the local Courant–Friedrichs–Lewy (CFL) numbers.

3.3. Nonlinear system

Among the methods available for extending the scheme described in the previous paragraph to nonlinear systems, the characteristic decomposition is the most common. This procedure is used to approximate the wave propagation locally. The characteristic equations are defined as

$$\alpha_t + \Lambda \alpha_x = 0 \tag{11}$$

where $\alpha = R^{-1}U$, $A = R\Lambda R^{-1}$, A is the Jacobian of the flux function and Λ is a diagonal matrix with the eigenvalues of A .

This approach is valid only if the eigenvalues of the flux Jacobian are real and distinct.

In order to avoid the characteristic decompositions and as specified by Liu and Lax [5] on the importance and potential of flux splitting approach, we write the 1D homogeneous nonlinear system as

$$\left(\frac{U}{J}\right)_t + \tilde{F}^+(U)_\xi + \tilde{F}^-(U)_\xi = 0 \tag{12}$$

Here, the splitting is based on the so-called local flux splitting [5]:

$$\tilde{F}(U) = \tilde{F}^+(U) + \tilde{F}^-(U) \tag{13}$$

To generalize scheme (10) and to achieve second-order accuracy in time we propose to use a second-order accurate Runge–Kutta method

$$\begin{aligned} U_j^* &= U_j^n - \lambda [J_{j+1/2} \tilde{F}_{j+1/2}^+ - J_{j-1/2} \tilde{F}_{j-1/2}^+ + J_{j+1/2} \tilde{F}_{j+1/2}^- - J_{j-1/2} \tilde{F}_{j-1/2}^-] \\ U_j^{**} &= U_j^* - \lambda [h_{j+1/2} - h_{j-1/2}] \\ U_j^{n+1} &= \frac{1}{2}U_j^n + \frac{1}{2}U_j^{**} \end{aligned} \tag{14}$$

The adapted numerical flux can be expressed as

$$\begin{aligned} h_{j+1/2} &= g_{j+1/2}^E + \frac{1}{2}\phi(r_j^+) (\Delta f_{j+1/2})^+ - \frac{1}{2}\phi(r_{j+1}^-) (\Delta f_{j+1/2})^- \\ \text{with } (\Delta f_{j+1/2})^+ &= J_{j+1/2} [\tilde{F}_{j+1}^{*+} - \tilde{F}_j^+] \quad \text{and} \quad (\Delta f_{j+1/2})^- = J_{j+1/2} [\tilde{F}_{j+1}^- - \tilde{F}_j^{*+}] \end{aligned} \tag{15}$$

For the 2D shallow-water system, we use the well-known dimension-by-dimension technique.

4. THE MOVING MESH METHOD

This section presents a moving mesh technique as introduced by Tang and Tang [6]. The adaptive moving mesh is generated by transforming the uniform mesh in the computational domain Ω_c to cluster grid points at the regions of the physical domain Ω_p , where the solution has large gradients. In what follows, we present the 1D version of the method.

4.1. Mesh adaptation

To derive the coordinate transformation, we use the equidistribution principle. The mesh map is provided by the minimizer

$$E(\xi) = \frac{1}{2} \int_{\Omega_p} \omega^{-1}(\xi_x)^2 dx \tag{16}$$

In practice, we solve the following equivalent equation:

$$(\omega x_\xi)_\xi = 0 \tag{17}$$

By using central difference approximations and Gauss–Seidel iteration we obtain the moving mesh equation:

$$\omega(u_{j+1/2}^{[v]})(x_{j+1}^{[v]} - x_j^{[v+1]}) - \omega(u_{j-1/2}^{[v]})(x_j^{[v+1]} - x_{j-1}^{[v+1]}) = 0 \tag{18}$$

4.2. Moving mesh algorithm

The following algorithm summarizes the crucial stages of the adaptive mesh method.

Algorithm

Determine an initial uniform mesh: $x_j^0 = x_L + j \frac{x_R - x_L}{N}$, $j = 0, \dots, N$.

while $t_n < T$ **do**

repeat

$v = 0$; $x_j^{[0]} = x_j^n$; $U_j^{[0]} = U_j^n$, $j = 0, \dots, N$.

 Solve the mesh redistribution equation by Gauss–Seidel iteration (18) to move grid $\{x_j^{[v]}\}$ to $\{x_j^{[v+1]}\}$.

 Interpolating the approximate solution U^n on the new grid.

until $v \geq v_{\max}$ or $\|x^{[v+1]} - x^{[v]}\| \leq \epsilon$

 Compute the solution one time step U^{n+1} using the high-resolution method (14).

end while

Remark

The method of interpolation is based on the conservative approach introduced by Tang and Tang [6]. This technique allows the resulting solution to satisfy the most fundamental properties relating to the conservation laws equations. The above algorithm preserves the monotonic order of $x^{[v]}$:

$$x_{j+1}^{[v]} > x_j^{[v]} \implies x_{j+1}^{[v+1]} > x_j^{[v+1]}, \quad j = 0, \dots, N$$

To avoid very singular meshes due to local gradient change, a regularization of the monitor function is applied $\omega_{j+1/2} \leftarrow \frac{1}{4}(\omega_{j-1/2} + 2\omega_{j+1/2} + \omega_{j+3/2})$.

5. NUMERICAL RESULTS

Multiple tests have been developed. In our computations, the CFL condition is

$$\max((|V_\xi| + \sqrt{gh\beta})\Delta t / \Delta \xi, (|V_\eta| + \sqrt{gh\gamma})\Delta t / \Delta \eta) \leq 0.4$$

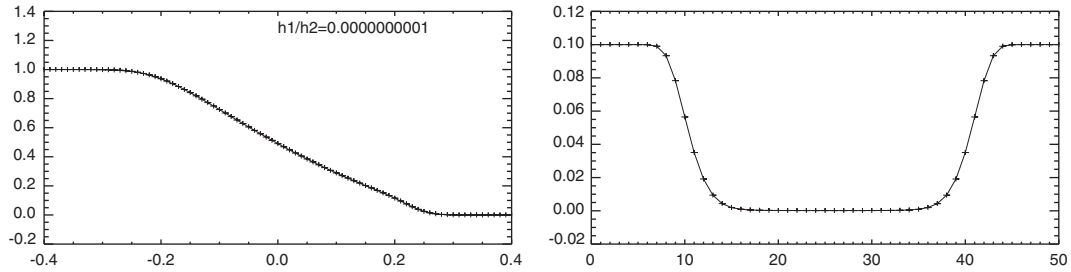


Figure 1. Heights of water flow for tests 1 and 2 for time $T=0.1$ and 5, respectively.

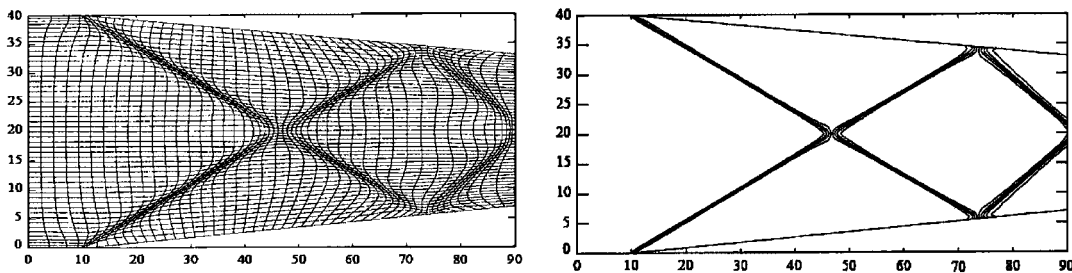


Figure 2. Geometry, mesh and contour plot of the steady solution for the symmetric channel constriction with 51×51 grid points.

where $V_\xi = uy_\eta - vx_\eta$, $V_\eta = vx_\xi - uy_\xi$, $\beta = \sqrt{x_\eta^2 + y_\eta^2}$ and $\gamma = \sqrt{x_\xi^2 + y_\xi^2}$.

5.1. Test 1: dam break problem

At time $t=0$, the barrier of a wide channel with $h_1=1$ and $h_2=10^{-10}$, the heights of the water upstream and downstream are suddenly removed. The flow consists of a bore traveling downstream and a rarefaction wave traveling upstream (Figure 1).

5.2. Test 2: generation of a dry bed

At time $t=0$, the conditions have been chosen in order to obtain two rarefaction waves separated by a dry bed. The water depth is 0.1 m and the initial velocity is 3 and -3 m/s on the left- and right-hand sides of the discontinuity, respectively. The latter is located at the channel mid-length.

5.3. Test 3: symmetric channel constriction

The channel wall is symmetrically constricted from both sides with angle $\alpha=5$. The initial and inflow conditions are the height $h_0=1$ and Froud number 2.5 (Figure 2).

6. CONCLUSION

We have presented a numerical scheme for SWE, which offers significant improvement over available methods in terms of simplicity, adaptability and resolution.

REFERENCES

1. Louaked M, Hanich L. TVD scheme for the shallow water equations. *Journal of Hydraulic Research* 1998; **36**:363–378.
2. Louaked M, Hanich L. TVD-multiresolution scheme for the shallow water equations. *Comptes Rendus de l'Académie des Sciences I* 2000; **331**:745–750.
3. Sweby PK. High-resolution schemes using flux limiters for hyperbolic conservation-laws. *SIAM Journal on Numerical Analysis* 1984; **21**:995–1011.
4. Harten A. High resolution schemes for hyperbolic conservation laws. *Journal of Computational Physics* 1983; **49**:357–393.
5. Liu X, Lax PD. Positive schemes for solving multi-dimensional hyperbolic systems of conservation laws II. *Journal of Computational Physics* 2003; **187**:428–440.
6. Tang H, Tang T. Adaptive mesh methods for one- and two-dimensional hyperbolic conservation laws. *SIAM Journal on Numerical Analysis* 2003; **41**(2):487–515.